




RESEARCH ARTICLE OPEN ACCESS

In Vivo Measurements Reveal Increased Nucleus Pulposus Lactate and Oxygen Concentrations in a Goat Model of Intervertebral Disc Degeneration

Karthikeyan Rajagopal^{1,2} | Thomas P. Schaer^{1,3}  | Kyle D. Meadows⁴ | Madeline Boyes³ | Rachel Hilliard³ | John C. O'Donnell^{5,6} | George R. Dodge² | Dmitriy Petrov⁵ | Dawn M. Elliott⁴  | Robert L. Mauck^{1,2} | Lachlan J. Smith^{1,2,5}  | Neil R. Malhotra^{1,2,5}

¹Translational Musculoskeletal Research Center, Corporal Michael J. Crescenz VA Medical Center, Philadelphia, Pennsylvania, USA | ²Department of Orthopaedic Surgery, Perelman School of Medicine, University of Pennsylvania, Philadelphia, Pennsylvania, USA | ³Department of Clinical Studies, New Bolton Center, School of Veterinary Medicine, University of Pennsylvania, Kennett Square, Pennsylvania, USA | ⁴Department of Biomedical Engineering, University of Delaware, Newark, Delaware, USA | ⁵Department of Neurosurgery, Perelman School of Medicine, University of Pennsylvania, Philadelphia, Pennsylvania, USA | ⁶Center for Neurotrauma, Neurodegeneration and Restoration, Corporal Michael J. Crescenz VA Medical Center, Philadelphia, Pennsylvania, USA

Correspondence: Lachlan J. Smith (lachlans@pennmedicine.upenn.edu) | Neil R. Malhotra (neil.malhotra@pennmedicine.upenn.edu)

Received: 25 September 2024 | **Revised:** 20 April 2025 | **Accepted:** 22 April 2025

Funding: This work was supported by National Institute of Arthritis and Musculoskeletal and Skin Diseases (P30AR069619, R01AR077435); U.S. Department of Veterans Affairs (I01RX001321, IK2RX003376, IK6RX003416).

Keywords: caprine | endplate | lumbar | metabolites | microdialysis | nutrition | oxygen probe

ABSTRACT

Introduction: Intervertebral disc degeneration is strongly implicated as a cause of low back pain. Although the precise pathophysiological mechanisms remain elusive, perturbations in nutrition that adversely impact the cellular microenvironment of the central nucleus pulposus (NP) may be contributing factors. A comprehensive understanding of this microenvironment, including changes in nutrient availability as a function of degeneration, is critical for the development of effective cell-based treatments. The goal of this study was to adapt brain tissue oxygen probes and microdialysis catheters for in situ determination of relative NP oxygen, glucose, and lactate levels in a preclinical goat model of disc degeneration.

Methods: Following ex vivo technical refinement in bovine caudal discs, baseline metabolite measurements were performed in vivo in the lumbar discs of 3 large frame goats. Degeneration was then induced via injection of chondroitinase ABC (ChABC) into the NP, and measurements were repeated after 12 weeks. Degeneration severity was graded using magnetic resonance imaging (MRI) and histology, and vertebral endplate porosity was assessed using microcomputed tomography.

Results: Oxygen and lactate levels in goat NPs were significantly higher in degenerate compared to healthy discs, while glucose levels were not significantly different. ChABC-injected discs exhibited higher vertebral endplate porosity, worse histological and MRI grades, and a spectrum of cartilage endplate damage compared to healthy discs. There were significant positive correlations between MRI grade and both NP oxygen and lactate levels.

Discussion: We successfully adapted techniques including surgical placement, equilibration time, flow rate, and detection method for in situ measurement of oxygen, glucose, and lactate in a goat model of disc degeneration. Interestingly, while increased lactate with degeneration was expected, increased oxygen levels were unexpected. Our findings may, in part, be explained by associated alterations in disc and endplate structure, and motivate future studies to comprehensively establish the underlying mechanisms in this model.

This is an open access article under the terms of the [Creative Commons Attribution-NonCommercial-NoDerivs](https://creativecommons.org/licenses/by-nc-nd/4.0/) License, which permits use and distribution in any medium, provided the original work is properly cited, the use is non-commercial and no modifications or adaptations are made.

© 2025 The Author(s). JOR Spine published by Wiley Periodicals LLC on behalf of Orthopaedic Research Society.

1 | Introduction

Chronic low back pain is a leading contributor to disability and imposes a substantial socioeconomic burden worldwide [1]. A key cause of low back pain is lumbar intervertebral disc degeneration [2, 3]. The intervertebral discs are the partially movable joints of the spine. Each disc is comprised of a central, gelatinous, proteoglycan-rich nucleus pulposus (NP), a peripheral, fibrocartilaginous annulus fibrosus (AF), and superiorly and inferiorly, two cartilaginous endplates (CEPs) that interface with the adjacent vertebrae [4, 5]. The primary function of the disc is mechanical and includes facilitating both the even transfer and distribution of forces between the vertebrae and, in concert with the posterior facet joints, complex multiaxial mobility of the intervertebral joint [4, 5]. Disc degeneration is a slowly progressing, cell-mediated cascade that is closely linked to aging [2, 6]. Although the precise pathophysiological mechanisms driving disc degeneration remain elusive, contributing factors may include reduced vascular supply and consequent alterations within the nutritional microenvironment, the disappearance of notochordal NP cells, mechanical trauma, genetics, comorbidities such as obesity and diabetes, and lifestyle [4, 7].

The earliest manifestations of disc degeneration typically occur in the NP, where altered cellularity and increased local inflammation drive extracellular matrix (ECM) changes that compromise biomechanical function [4, 8]. The NP is an avascular tissue, and resident cells largely depend on capillaries located in the underlying vertebral endplates (VEPs) for the provision of critical metabolites such as oxygen and glucose, which diffuse through the CEPs [9]. Metabolic waste secreted by NP cells diffuses from the disc in the opposite direction and creates a concentration gradient depending on the rates of nutrient supply and cell metabolism. Diminished nutrient supply to the NP has long been considered a trigger for disc degeneration [10]. Studies tracking the diffusion of paramagnetic contrast media using MRI showed reduced diffusion in mildly degenerated discs [11]. Morphological assessments of the VEPs showed that with increased degeneration severity, there was a decrease in pore density, particularly of those that hold capillary buds [12]. Pathological occlusion of endplate pores may result in an inadequate nutrient supply and increased NP tissue acidity due to lactate accumulation, both of which negatively impact NP cell viability and ECM production [13]. There has been a lack of appropriate *in vivo* models as well as sufficiently sensitive quantitative techniques for *in situ* assessment. Consequently, very few studies have performed direct, *in situ* measurements of NP metabolite concentrations in healthy and degenerated discs.

Currently, low back pain is most often managed conservatively, while patients with advanced disc degeneration may be treated surgically using procedures such as spinal fusion or total disc replacement [14]. These interventions may provide symptom relief but fail to restore healthy disc structure and mechanical function, and exhibit poor long-term efficacy [15]. Emerging cell-based treatments such as those using mesenchymal stem cells (MSCs) have shown the potential to regenerate NP tissue, relieve discogenic pain, and prevent disc degeneration progression [16–18]. However, the degenerate NP microenvironment poses a major challenge to effective cell-based treatment, as limited oxygen and nutrient supply adversely affect the performance of

therapeutic cells [19, 20]. This challenge is compounded by our limited understanding of the dynamic nutritional microenvironment of the degenerating disc.

Microdialysis is widely used to monitor cerebral glucose and other metabolite levels in patients with acute brain injury due to trauma or ischemic stroke [21]. The procedure involves atraumatic insertion of a catheter into the brain parenchyma, through which isotonic fluid is circulated. A semipermeable membrane at the tip of the catheter functions like a blood capillary, allowing small molecules and solutes in the extracellular fluid of the tissue to diffuse across it, depending on their size and concentration [21]. Subsequently, the perfusion fluid passing through the catheter captures these molecules, exits as dialysate, and is collected in a micro-vial for analysis. The Licox system is a pre-calibrated Clark-type oxygen probe, which is commonly used to monitor cerebral oxygen levels in patients with acute brain injury [22]. The probe consists of two electrodes covered with a gas-permeable membrane. In the targeted tissue, soluble oxygen diffuses through the membrane and is electrochemically reduced at one of the electrodes, generating an electric current [22]. The change in voltage between the reference and measuring electrodes is directly proportional to the tissue oxygen concentration, but this relationship varies depending on temperature. For this reason, the probes also contain an integrated thermocouple that provides continuous tissue temperature to the monitor for use in calculating and displaying real-time tissue oxygen.

Given that nutrient diffusion to the center of the disc is a function of size, especially disc height, physiologically relevant characterization of the disc microenvironment requires selection of an appropriate animal model [10]. Compared to rodents, larger animals such as goats, sheep, pigs, and dogs have discs that more closely approximate the geometry and nutritional microenvironment of human discs. We and others have previously described a lumbar disc degeneration model in goats using intradiscal injection of chondroitinase ABC (ChABC) [23, 24]. This model recapitulates clinically relevant degeneration characteristics observed in humans, such as loss of proteoglycans, reduced disc height, alterations in VEP morphology, compromised biomechanics, and elevated pro-inflammatory cytokine expression [23, 25]. The objective of this study was to adapt brain tissue oxygen probes and microdialysis techniques to determine relative NP oxygen, glucose, and lactate levels in healthy and degenerate intervertebral discs in a preclinical goat model.

2 | Methods

2.1 | Ex Vivo Technical Refinement

Prior to conducting oxygen, glucose, and lactate measurements in live animals, techniques were refined *ex vivo* using a bovine caudal disc model (Figure 1A). Three adult bovine tails were obtained within 24 h of death (Research 87 Inc.; Boylston, MA, USA), and musculature and other soft tissues were removed to expose the coccygeal discs between C1 and C5. Oxygen measurements were performed using the Licox Brain Tissue Oxygen Monitoring System (Integra Lifesciences; Princeton, NJ, USA). A 16G×1.5-in. needle was used to position a Licox

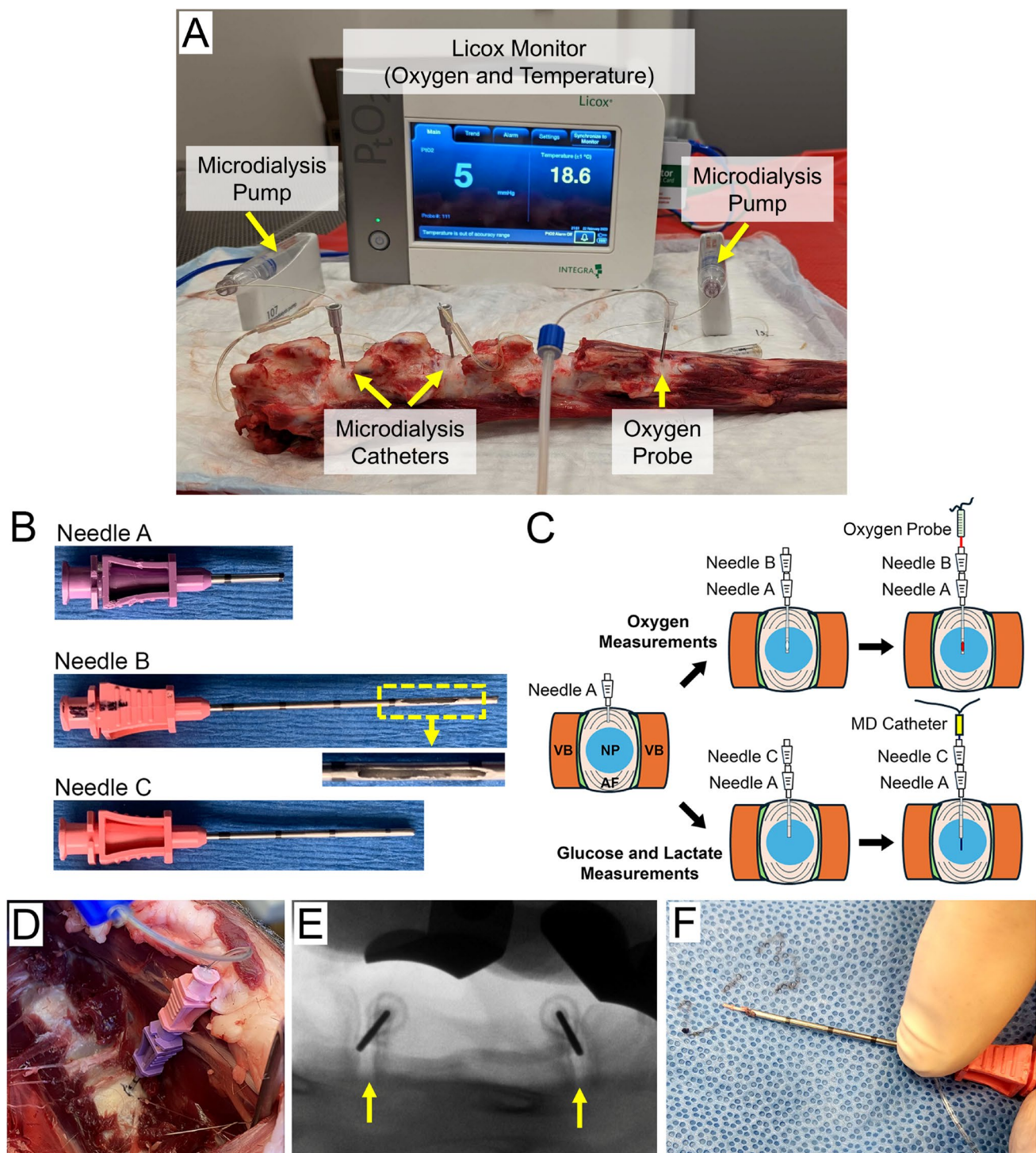


FIGURE 1 | (A) Experimental setup for ex vivo oxygen and microdialysis measurements using bovine caudal discs. (B) Customized spinal needles used for in vivo probe placement. Inset shows window machined into Needle B to expose the oxygen probe to the tissue microenvironment. (C) Schematic showing needle assembly and placement for oxygen and microdialysis (MD) measurements. (D) Needle assembly positioned in a goat lumbar disc. (E) Representative lateral fluoroscopy image showing probes placed in two adjacent discs (arrows). (F) Undamaged microdialysis catheter following retrieval.

probe (pre-calibrated by the manufacturer) in the center of the NP of each disc, with placement confirmed using fluoroscopy. Oxygen levels (mmHg) in $n=4$ discs were recorded at 5-min time intervals for 90 min. Glucose and lactate contents were measured using microdialysis. A Brain Microdialysis CMA 70 catheter with a membrane length of 10 mm and a molecular

cut-off of 20 kDa (M Dialysis AB, Stockholm, Sweden) was used. Isotonic perfusion fluid (147 mmol/L NaCl, 2.7 mmol/L KCl, 1.2 mmol/L CaCl_2 , and 0.85 mmol/L MgCl_2) used for cerebral microdialysis was pumped into the catheter using a perfusion pump (CMA 107; M Dialysis) at one of two flow rates: 0.3 or $1 \mu\text{L}/\text{min}$ ($n=3$ discs each). Following initial system priming

and equilibration, microdialysates were collected in micro-vials at 30-min time intervals for 150 min. Glucose and lactate levels in the microdialysates were determined using two independent assay types: the clinical ISCUSflex Microdialysis Analyzer (M Dialysis) that enables multiplex analysis of multiple metabolite types in a single sample, and high-sensitivity, single-analyte detection kits for glucose (Sigma, St. Louis, MO, USA) and lactate (Abcam, Cambridge, MA, USA). In both instances, results were expressed in mmol/L. Accuracy of microdialysis measurements was assessed using whole disc organ culture. A bovine caudal disc with intact cartilage endplates was cultured under limited swelling conditions as described previously [26], in high glucose Dulbecco's Modified Eagle Medium supplemented with 10% fetal bovine serum, ascorbic acid (50 µg/mL) and 1% antibiotic-antimycotic (all from Thermo Fisher Scientific, Waltham, MA, USA). After 7 days of culture, a microdialysis catheter was positioned in the NP as described above, and, following priming and equilibration, microdialysates were collected at 30-min time intervals for 150 min at a flow rate of 0.3 µL/min. Glucose concentrations in the microdialysates and culture media ($n = 3$ aliquots) were measured using a high-sensitivity detection kit.

2.2 | In Vivo Measurements in a Goat Model of Disc Degeneration

Animal experiments were approved by the Institutional Animal Care and Use Committees of the University of Pennsylvania and the Corporal Michael J. Crescenz VA Medical Center. Three skeletally mature, large-frame goats (male castrated mixed breed Nubian crosses, approximately 4 to 6 years old; Thomas D. Morris Inc., Reisterstown, MD, USA) were used in this study. All 3 goats underwent two surgical procedures, 12 weeks apart. During the first surgery, under general anesthesia, the lumbar intervertebral discs (L1–L6) were exposed using a left lateral retroperitoneal transpossoatic approach, as described previously [23]. During placement, probes were found to self-eject from the disc due to the high swelling pressure of the NP, an issue not encountered during ex vivo measurements. To address this challenge, guide needles were further customized. Specifically, we utilized three customized coaxial anchoring spinal needles (GeoTeck Health Care Products, Ankara, Turkey; needles “A,” “B,” and “C,” shown in Figure 1B,C). To prevent damage to the probes, bevels were first blunted using grinding discs. Needle A (15G×18mm) served as an anchor within the AF. Depending on the probe type (Licox oxygen probe or microdialysis catheter), we then inserted either Needle B or C through Needle A (Figure 1C,D). For oxygen analysis, we used Needle B (17G×58.5 mm), which was modified with an 8 mm side opening to expose the Licox probe to soluble oxygen in the tissue while protecting it from damage. After positioning the probe, the needle port was sealed with bone wax to prevent atmospheric oxygen from impacting the measurements. For microdialysis, where 360° contact of the catheter with the NP tissue was imperative, Needle C (17G×48 mm) was used. Accurate probe placement within the NP was confirmed using 3D fluoroscopic imaging with an ARCADIS Orbic 3D mobile C-arm system that provides fast scan times (Siemens Medical Solutions USA Inc., Malvern, PA, USA) (Figure 1E), and baseline measurements were collected from 7 discs. Probe integrity was confirmed at the completion of measurements following retrieval

from the disc (Figure 1F). Oxygen measurements were recorded at 5-min intervals for 30 min ($n = 7$ discs at baseline). While this was shorter than for ex vivo studies, a preliminary assessment using cadaveric goat lumbar discs and subsequent in vivo confirmation in two discs at 12 weeks (Figure S1) indicated faster equilibration than for bovine tail discs, and this shorter period of collection facilitated a reduction in surgery time. For glucose and lactate measurements, microdialysis catheters were perfused with isotonic fluid at a flow rate of 0.3 µL/min. Following initial priming and equilibration, microdialysates were collected at 30-min intervals up to 150 min ($n = 5$ discs at baseline). Subsequently, intervertebral disc degeneration was induced by injecting 2 U of ChABC (Amsbio; Cambridge, MA, USA) resuspended in 200 µL of phosphate buffered saline containing 0.1% bovine serum albumin into the NPs of 4 or 5 discs (L1–L6), while the T13–L1, L1–2, and/or L6–L7 discs served as intact healthy controls. After allowing degeneration to progress for 12 weeks, a second surgery was performed, where Licox and microdialysis measurements were repeated ($n = 6$ discs each for both measurement types). Note that sample sizes were inconsistent at baseline versus 12 weeks due to probe damage occurring during placement (noted during the probe integrity check at the completion of measurements) that resulted in failed measurements for some discs. Additionally, the isolated impact of probe insertion alone on disc degeneration was assessed. Specifically, a subset of discs ($n = 4$) received ChABC injections but did not undergo probe insertion and monitoring at either time point.

The glucose and lactate concentrations in microdialysates were determined using the single analyte high-sensitivity detection kits described above. In vivo magnetic resonance images (MRI) and lateral plain radiographs of the lumbar spine were obtained at 0 weeks (before the first surgery) and again at 12 weeks (prior to the second surgery). Mid-sagittal T2-weighted images were obtained using a 3T clinical MRI scanner (Siemens Magnetom TrioTim; Munich, Germany), and disc degenerative condition at 12 weeks (intact, ChABC only and ChABC plus probes) was assessed using semiquantitative Pfirrmann grading by three independent observers blinded to the study groups (results averaged prior to statistics). Disc height index (DHI) at 12 weeks as a percentage of baseline was determined from radiographs using established techniques [27]. Following the second surgery, animals were euthanized using an overdose of sodium pentobarbital solution following American Veterinary Medical Association guidelines. Lumbar spines were then harvested for the postmortem analyses described below.

2.3 | Microcomputed Tomography and Histology

Lumbar spines were flensed of surrounding musculature, and posterior bony elements were removed. Vertebra-disc-vertebra spine segments were prepared by cutting through intervening vertebral bodies, fixed in buffered 10% formalin for 1 week at 4°C, and then imaged using microcomputed tomography (µCT) (MicroCT45; Scanco Medical, Switzerland) at an isotropic resolution of 24.2 µm, an energy of 70 kVp, a current of 114 µA, and a 250 ms integration time. 3D images were reconstructed using Scanco software and manually segmented to visualize the surfaces of the cranial and caudal VEPs. Percent porosity of the VEP surfaces was calculated using ImageJ software (Version 1.53t;

National Institutes of Health, Bethesda, MD, USA). Results for cranial and caudal VEPs were averaged prior to statistics.

Following μ CT imaging, spine segments were decalcified in formic and ethylenediaminetetraacetic acids (Formical 2000; StatLab; McKinney, TX, USA) for 4 weeks and processed for paraffin histology. Mid-sagittal, $8\mu\text{m}$ sections were cut and double stained with either Alcian blue and picosirius red to demonstrate glycosaminoglycans and collagen, respectively, or hematoxylin and eosin to demonstrate cellularity. Stained sections were imaged using an AxioScan.Z1 slide scanner (Carl Zeiss AG; Oberkochen, Germany) at $10\times$ magnification. Semiquantitative grading of disc degenerative condition was graded by three independent observers (results averaged prior to statistics), using an adaptation of established techniques (Table S1) [23, 28]. Five categories were assessed on a scale of 0 (normal) to 100 (severely abnormal): (1) organization of the AF, (2) NP matrix, (3) demarcation of the AF/NP border, (4) NP cellularity, and (5) CEP structure. An overall grade for each disc was calculated as the sum of these individual parameters.

2.4 | Statistical Analyses

Statistical analyses were performed using Prism (v8.3.0; GraphPad Software; San Diego, CA, USA). Results are reported as median and interquartile range (IQR). For in vivo oxygen measurements, statistical comparisons were performed on instantaneous values measured at 30 min. For glucose and lactate, statistical comparisons were performed on averaged results for microdialysates collected at the final 3 collection time points: 90, 120, and 150 min (to ensure fully stable and equilibrated measurements). Mann–Whitney U tests were used for all pairwise comparisons. For ex vivo microdialysis measurements, Kruskal–Wallis tests with post hoc Dunn's tests were used to establish the effect of flow rate and assay type on results. The impact of ChABC injection (with and without probe placement) on degeneration severity at 12 weeks assessed using Pfirrmann grade, VEP porosity, and histology grade was established using Kruskal–Wallis tests with post hoc pairwise Dunn's tests. Changes in disc height at 12 weeks relative to baseline following ChABC injection (with and without probe placement) were determined using Wilcoxon signed rank tests. Correlations between glucose, lactate, and oxygen levels and MRI Pfirrmann grade were determined using Spearman's tests. Significance was defined as $p < 0.05$ for all tests.

3 | Results

3.1 | Ex Vivo Refinement

Licor and microdialysis acquisition parameters were first evaluated using an ex vivo bovine caudal disc model (Figure 1). After positioning Licor probes in the NP, oxygen tension gradually decreased and equilibrated after approximately 45 min at 2 (5.75) mmHg ($\sim 0.109\text{ mol/m}^3$) (Figure 2A; note that the Licor system reports whole integers only; value in brackets is IQR). Microdialysis was performed at two different perfusion rates to determine the flow rate that provided the greatest recovery of metabolites from the interstitial fluid of the NP. For both flow

rates, metabolite measurements were relatively stable from approximately 30 min onwards (Figure 2B–E). Microdialysates collected at $0.3\mu\text{L/min}$ exhibited a higher recovery of metabolites compared to $1\mu\text{L/min}$, though the differences were not statistically significant (Figure 2C,E). We compared two different analytical techniques for measuring glucose and lactate concentrations: a clinical ISCUS analyzer and single analyte high-sensitivity detection kits. For $0.3\mu\text{L/min}$ flow rate samples (averaged microdialysates collected at 90, 120, and 150 min) assessed using the ISCUS analyzer, median glucose and lactate levels were 0.465 (0.673) mmol/L and 5.379 (4.983) mmol/L, respectively (Figure 2C,E). For single analyte kits, median glucose and lactate levels were 0.383 (0.871) mmol/L and 4.100 (4.983) mmol/L, respectively. While the single analyte kit measurements in the $0.3\mu\text{L/min}$ flow rate samples were lower than those measured using the ISCUS system, the differences were not statistically significant. For the $1\mu\text{L/min}$ flow rate, values were similar for both assay methods for glucose and lactate. Finally, the glucose concentration in microdialysates collected from whole disc organ culture was 25.432 (1.094) mmol/L (median of 90, 120, and 150 min collection time points), which was 89.5% of the concentration measured in the culture media (28.425 (0.277) mmol/L).

3.2 | In Vivo Measurements in a Goat Model of Disc Degeneration

In vivo MRI and plain radiography were performed to confirm the presence and severity of disc degeneration following ChABC injection, and examine any additional impact of probe placement. Qualitatively, T2-weighted, mid-sagittal MRI images showed signal intensity changes consistent with moderate to severe degeneration in ChABC discs after 12 weeks. Noted changes included reduced signal intensity in the NP and diminished disc height compared to both baseline for the same disc levels, and adjacent healthy, intact discs at 12 weeks (Figure 3A). Subjectively, ChABC discs that received probes exhibited similar degenerative changes to those that did not. Semiquantitative evaluation using Pfirrmann grading confirmed significantly higher ($p < 0.001$) grades for the ChABC-injected discs (both with and without probe placement) compared to healthy discs (Figure 3B). Pfirrmann grades for ChABC discs that received probes were not significantly different from those that did not. With respect to disc height, discs that received ChABC injections plus probe placement showed a significant decrease in DHI at 12 weeks compared to baseline (Figure 3C,D). For discs that received ChABC only, DHI was similarly decreased, but changes did not reach statistical significance.

In healthy discs at baseline, median oxygen after 30 min of equilibration was 50 (27) mmHg ($\sim 2.61\text{ mol/m}^3$, Figure 4A). In degenerate discs, 12 weeks after ChABC injection, median oxygen was 108 (50.25) mmHg ($\sim 5.65\text{ mol/m}^3$), which was significantly higher ($p = 0.02$) than healthy discs at baseline. Glucose and lactate results from microdialysates collected at 90, 120, and 150 min were averaged prior to statistics. For healthy discs at baseline, median glucose and lactate concentrations were 0.063 (0.071) mmol/L and 0.069 (0.102) mmol/L, respectively (Figure 4B,C). In degenerate discs after 12 weeks, median glucose was 0.104 (0.665) mmol/L (not significantly different from

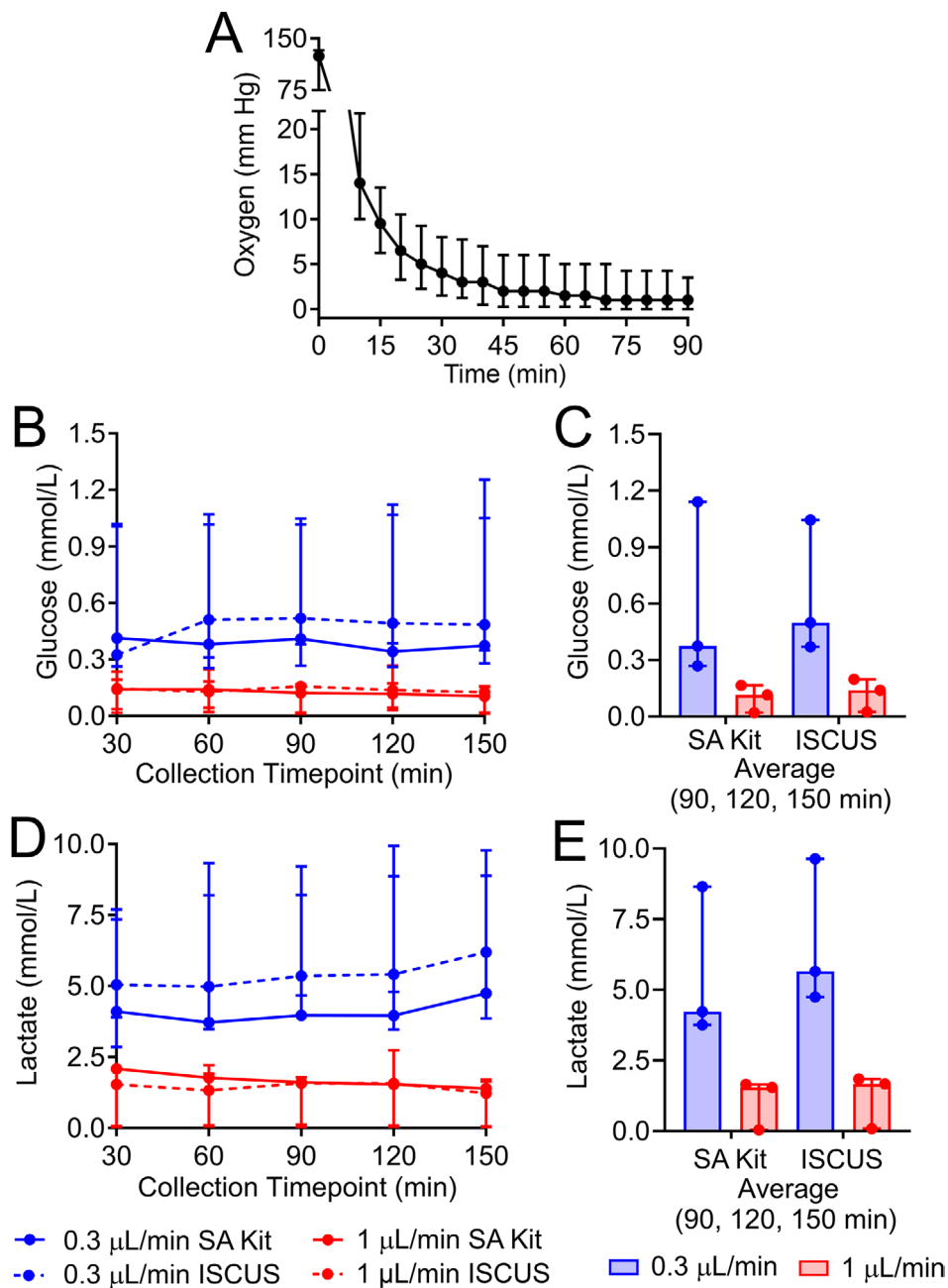


FIGURE 2 | (A) Ex vivo oxygen measurements in bovine caudal NPs over time. (B) Ex vivo glucose measurements over time as a function of flow rate and assay type. (C) Glucose measurements averaged for 90, 120, and 150 min collection time points. (D) Lactate measurements over time as a function of flow rate and assay type. (E) Lactate measurements averaged for 90, 120, and 150 min collection time points. $N=4$ (oxygen) and $N=3$ (glucose and lactate). Median and interquartile range. SA, single analyte.

baseline), and median lactate was 0.883 (1.981) mmol/L (significantly higher than baseline, $p=0.004$, Figure 4B,C).

3.3 | Microcomputed Tomography and Histology

Vertebral bony endplates adjacent to healthy and degenerate discs after 12 weeks were evaluated using μCT imaging (Figure 5). Subjectively, VEP bony erosion ranging from moderate to severe was evident adjacent to ChABC-injected discs (Figure 5A), and quantitative analysis revealed significantly higher porosity for discs that received ChABC plus

probes compared to healthy discs (Figure 5B). There were no significant differences in porosity between VEPs adjacent to ChABC-injected discs that received probe placement versus those that did not. Histological assessment revealed moderate-to-severe degeneration in ChABC-injected discs (Figure 6A,B). Subjectively, these discs exhibited reduced glycosaminoglycan staining in the NP and a less distinct AF/NP border compared to healthy discs. In addition, cartilaginous and vertebral bony endplate damage was observed, and in some instances was associated with herniation of disc tissue into the adjacent vertebrae. Semi-quantitative histological grading revealed that AF organization, NP matrix, AF/NP

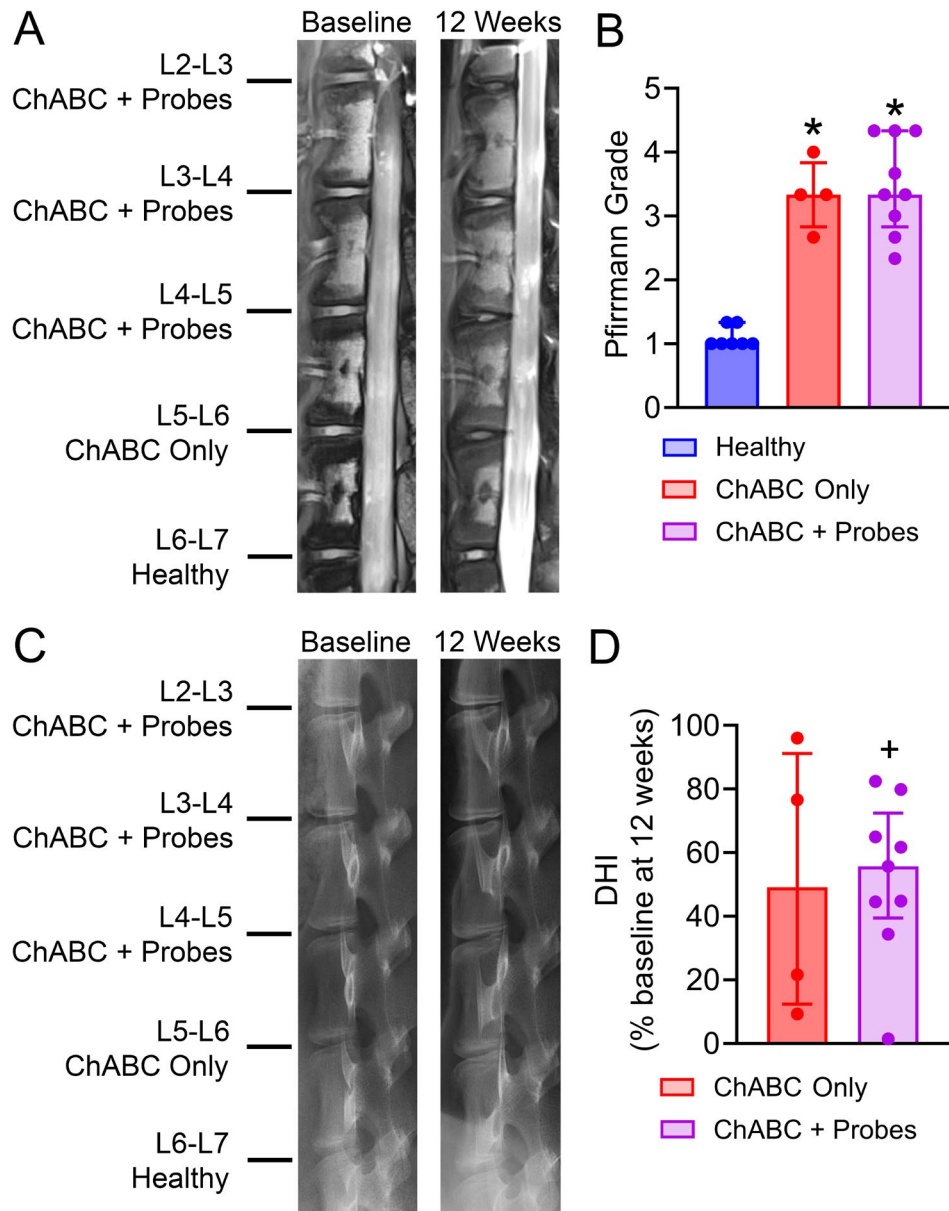


FIGURE 3 | (A) Representative in vivo, T2-weighted, mid-sagittal MRI images of a goat lumbar spine taken at baseline and 12 weeks after ChABC injection. (B) Semi-quantitative MRI grading of disc condition at 12 weeks. * $p < 0.05$ vs. healthy. (C) Representative in vivo radiographs of a goat lumbar spine taken at baseline and 12 weeks after ChABC injection. (D) Percentage change in disc height index (DHI) 12 weeks after ChABC injection compared to baseline (+ $p < 0.05$). $N = 4-9$; median and interquartile range.

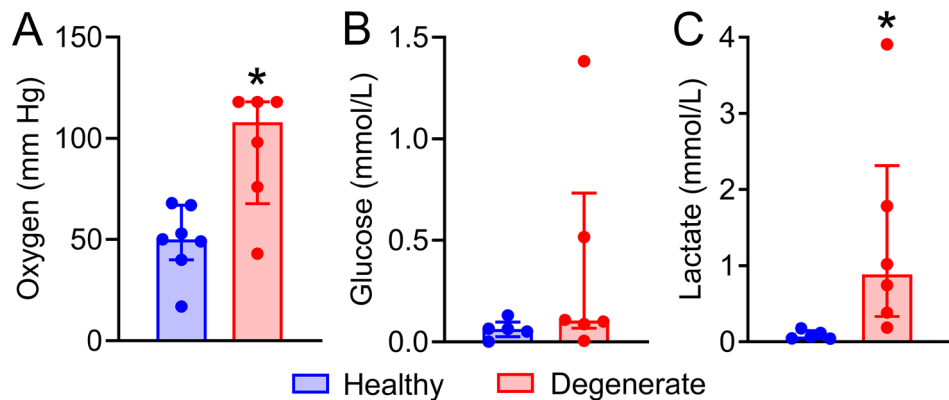


FIGURE 4 | (A) Oxygen, (B) Glucose, and (C) Lactate measured in vivo in healthy and degenerate goat NPs. Glucose and lactate are averaged for 90, 120, and 150 min collection time points. * $p < 0.05$ versus healthy; $N = 5-7$; median and interquartile range.

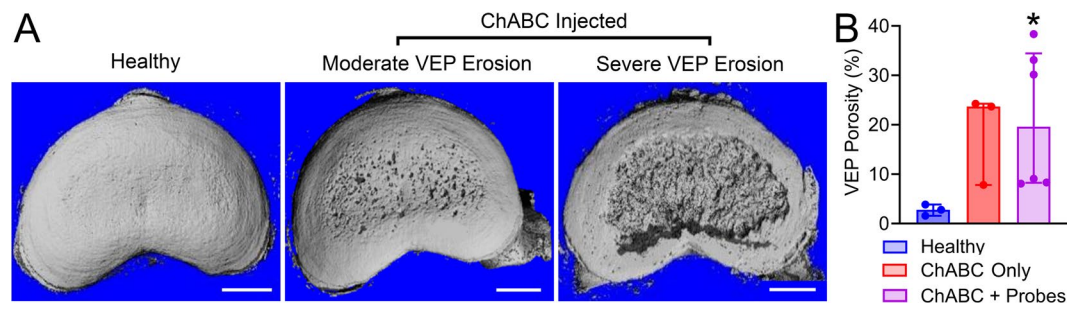


FIGURE 5 | (A) Representative μ CT images of vertebral endplates showing moderate to severe bony erosion adjacent to ChABC-injected discs. (B) Quantification of bony endplate porosity. * $p < 0.05$ versus healthy; $N = 3-6$; median and interquartile range.

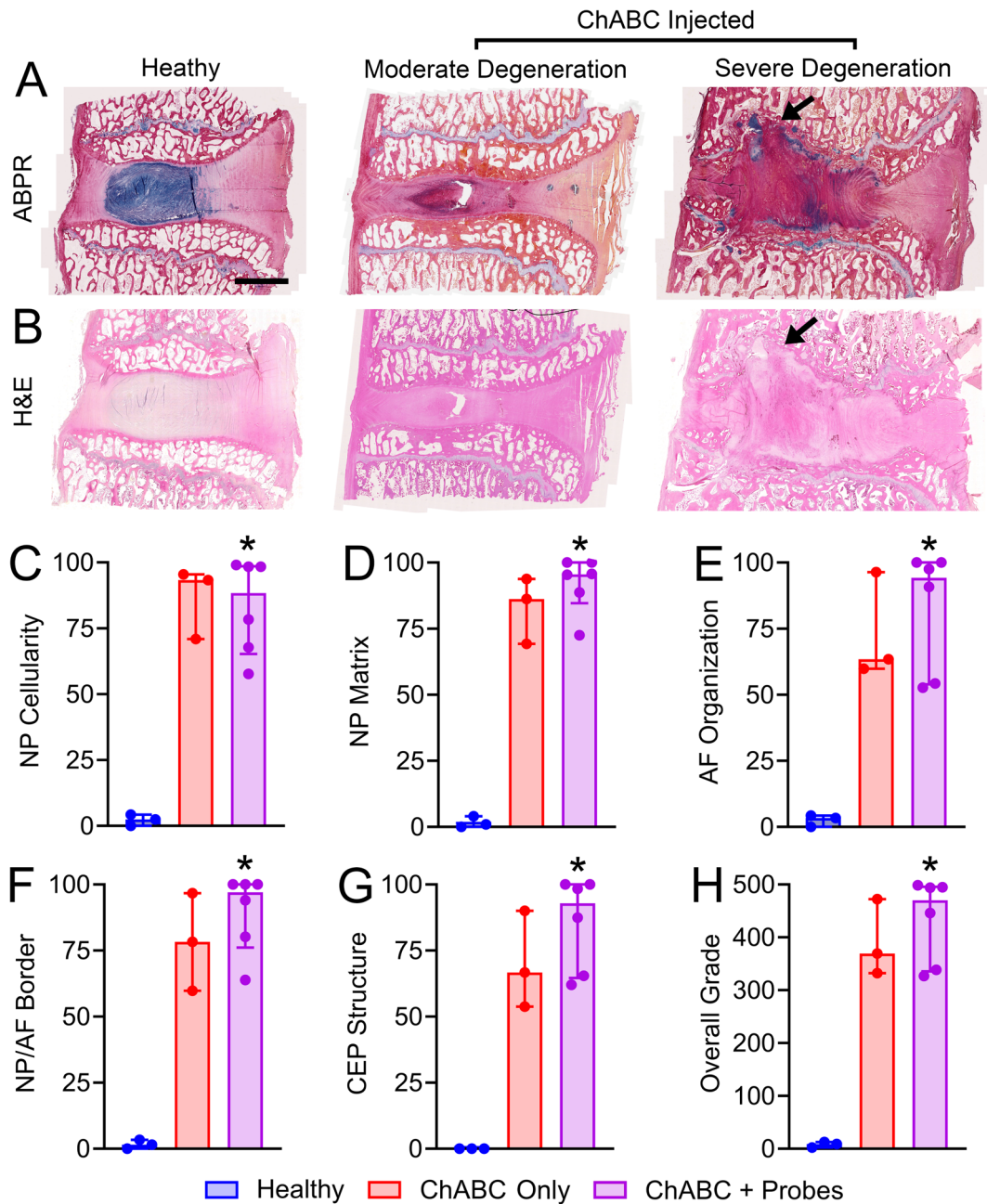


FIGURE 6 | (A) Representative Alcian blue and picosirius red (ABPR) and (B) hematoxylin and eosin (H&E) stained mid-sagittal histological sections of healthy and degenerate goat discs; scale = 5 mm. Note the presence of endplate damage and associated eruption of disc tissue into adjacent vertebrae in the severely degenerate disc (arrow). (C–G) Semi-quantitative histological grading of NP cellularity, NP matrix, AF organization, AF/NP border, and CEP structure. (H) Overall histological grade. * $p < 0.05$ versus healthy; $N = 3-6$; median and interquartile range.

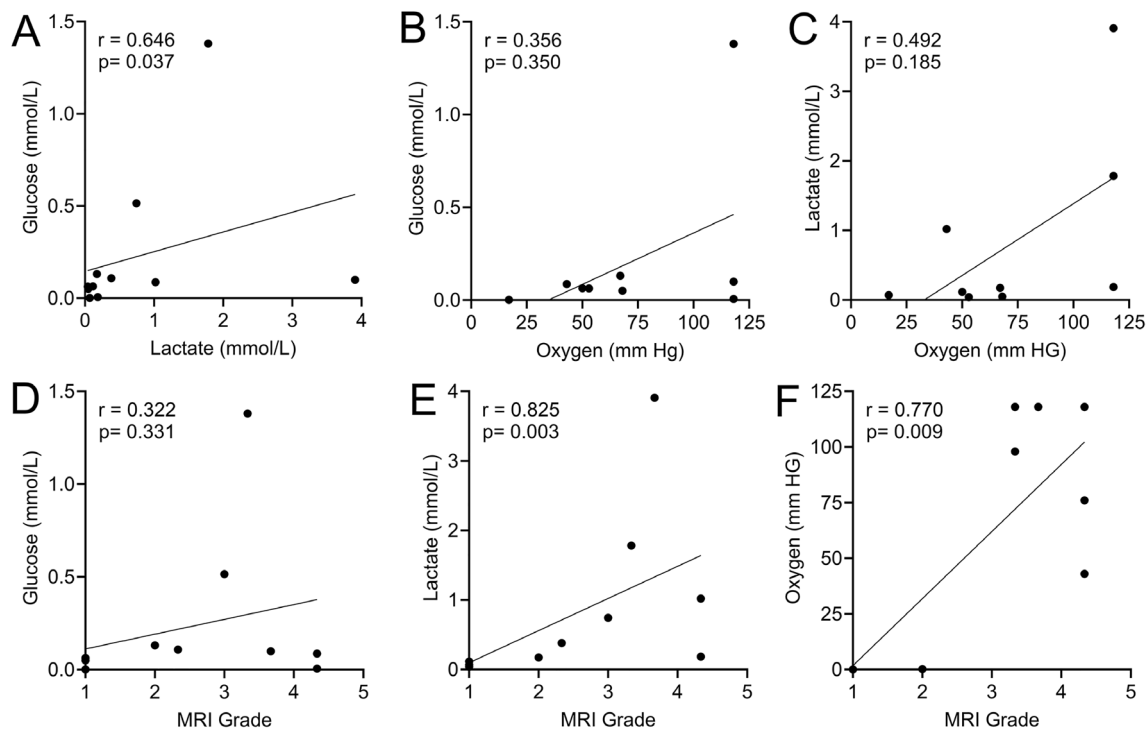


FIGURE 7 | Correlations (Spearman) between: (A) Glucose and lactate; (B) glucose and oxygen; and (C) lactate and oxygen measured in vivo in goat NPs (pooled healthy (baseline) and degenerate (12 weeks)). Correlations (Spearman) between disc MRI grade and: (D) glucose; (E) lactate; and (F) oxygen. $N=9-11$.

border, NP cellularity, EP structure, and overall grade were all significantly higher in ChABC-injected discs that received probes compared to healthy discs (Figure 6C–H). While some grading parameters were higher for ChABC discs that received probes compared to those that did not, there were no significant differences.

Finally, we examined correlations between glucose, lactate, and oxygen levels, and MRI Pfirrmann grade (Figure 7). Glucose levels were significantly and positively correlated with lactate levels ($r=0.646$, $p=0.037$, Figure 7A). Lactate and oxygen levels were both significantly and positively correlated with MRI grade ($r=0.825$, $p=0.003$; and $r=0.770$, $p=0.009$, respectively, Figure 7E,F).

4 | Discussion

Changes in the cellular microenvironment of the disc NP due to altered nutrient availability have long been considered to be major contributing factors to disc degeneration [29]. In this study, we adapted state-of-the-art in situ tools to investigate the in vivo nutritional microenvironment of the NP in both healthy and degenerate discs using a goat model. Disc degeneration was associated with significantly higher oxygen and lactate concentrations, and this occurred concomitantly with CEP damage and increased vertebral bony endplate porosity.

Historically, metabolite concentrations in the disc have been studied ex vivo, for example using surgical waste tissue obtained from discectomy, and relatively few have performed direct, in vivo measurements [30–34]. Bartels et al. measured in vivo

oxygen in human discs using chronoamperometry-based electrodes, but found no significant differences between patients with disc degeneration and scoliosis, and results were highly variable, ranging from 7.8 to ~140 mmHg [32]. Evaluation of oxygen levels in healthy canine discs using polarographic electrodes measured levels ranging from 0 to 16 mmHg [35]. Two prior studies used microdialysis to evaluate metabolite concentrations in vivo in healthy porcine lumbar and cervical discs, measuring concentrations of ~0.5 and ~2.5–4 mmol/L for glucose and lactate, respectively [30, 31]. For our studies, we used a goat ChABC-mediated model of disc degeneration. We previously showed that this model exhibits key characteristics of human degeneration, including clinically relevant structural, biomechanical, compositional, and inflammatory changes [23, 25]. More broadly, goat discs exhibit greater lumbar disc height (leading to greater diffusion distances) compared to other species of similar size (such as pigs and sheep) [36]. Also, like humans, these goat discs exhibit rapid loss of metabolically active notochordal NP cells by skeletal maturity (unlike some pig breeds and chondrodystrophic dogs, for example) [37]. Each of these characteristics could reasonably be expected to impact the nutritional microenvironment of the NP and help justify the selection of goats as a species for conducting these studies.

Our initial technical refinement studies were performed in bovine tail discs, focusing on parameters including probe placement, equilibration time, microdialysis flow rate, and detection methods for glucose and lactate. For microdialysis, we compared two flow rates based on prior literature [31, 38]. High flow rates decrease collection time, but may result in insufficient time for tissue metabolites to equilibrate within the perfusion fluid, leading to an underestimation of metabolite concentrations in

dialysates. High flow rates may also result in dilution of tissue metabolites, resulting in further underestimation. Conversely, lower flow rates increase collection time, but may enable more accurate measurements that are representative of the actual metabolite concentrations of the tissue. This was supported by our ex vivo findings, where a lower flow rate of 0.3 $\mu\text{L}/\text{min}$ resulted in higher levels of glucose and lactate detectable in microdialysates, with results comparable to previously reported measurements [30, 31]. Ex vivo experiments established an appropriate balance between diffusion time and collection volume for subsequent in vivo experimentation. Notably, for 1 $\mu\text{L}/\text{min}$, glucose levels were below the detectable limit of the ISCUS analyzer for some discs. While even lower flow rates are possible and may produce even more accurate readings, the corresponding increase in acquisition (and surgery) time made this impractical for in vivo experiments in anesthetized animals. To further improve measurement accuracy, we used high-sensitivity single-analyte assay kits to determine glucose and lactate contents in dialysates.

For in vivo studies, MRIs and radiographs confirmed that ChABC injection effectively induced disc degeneration after 12 weeks. Importantly, probe placement did not appear to significantly exacerbate the severity of degeneration compared to discs that received ChABC injection alone. Unlike in vitro assessments, during in vivo measurements, we encountered additional technical hurdles, primarily due to the higher NP swelling pressure and the narrow surgical corridor required to safely access the goat disc. Additionally, the absence of adjacent tissue structures for anchoring the probes (compared to the brain for example, where probes are anchored to the skull) posed a challenge. These factors resulted in the fragile Licox probes and microdialysis catheters being easily damaged or ejected from the disc and requiring replacement. To address these challenges, we used modified needles to position both probe types and maintain continuous contact with NP tissue.

With respect to in vivo findings, NP oxygen levels in healthy discs were of a similar order of magnitude to those reported previously for the goat NP [39]. Interestingly, compared to in vivo goat disc measurements, oxygen levels in the ex vivo bovine tail discs were lower and approached zero for some discs. A potential explanation for this discrepancy could be attributed to the function of the Licox probe, where the oxygen in the tissue is reduced by the cathode electrode, generating an electric current that determines the partial oxygen pressure. Due to the lack of active blood circulation in the bovine tail disc, the limited available oxygen may have been reduced and almost completely depleted by the electrode. In contrast, during in vivo testing, higher measurements may be due to the continuous diffusion of oxygen to the disc via the endplates from active blood circulation. Interestingly, both glucose and lactate contents were lower in healthy goat NP tissue compared to both our ex vivo bovine disc measurements and values reported in the literature [30, 31]. The reasons for this discrepancy are unknown; as discussed above, lower flow rates for microdialysis could potentially result in higher measurement values but are impractical due to the increased surgery time. Future studies could validate these in vivo readings against measurements made ex vivo on tissue samples to ascertain relative recovery of metabolites from the extracellular fluid.

In degenerate discs, both NP oxygen and lactate levels were significantly higher than in healthy discs and positively correlated with MRI grade, which was an unexpected finding. Capillary buds in the VEPs are the primary source of nutrients for the NP [10]. From these capillary buds, small molecules such as glucose and oxygen selectively diffuse across the CEPs into the NP [40]. Changes in the ECM composition and structure of the CEPs therefore have a direct impact on the metabolic microenvironment of the NP and the survival and performance of resident cells. Imaging studies have demonstrated diminished contrast agent diffusion across the CEP in degenerated discs [41], while ultrastructural studies have shown increased calcification and occlusion of CEP openings in degenerated discs [12, 42]. These findings suggest that disc degeneration is associated with decreased metabolite diffusion across the CEP and into the NP, resulting in reduced oxygen and glucose levels and higher lactate accumulation, given that NP cells produce lactate as metabolic waste as a byproduct of anaerobic glycolysis leading to increasing tissue acidity [10]. In the current study, the reasons for the apparently contradictory findings of elevated lactate and oxygen levels are unclear. Notably, a previous study found that some patients with back pain exhibited higher oxygen levels in degenerated discs [32]. Prior work in human cadaveric discs showed that endplate defect size is positively correlated with the severity of disc degeneration and negatively correlated with intradiscal pressure [43]. Furthermore, it has been shown that the total endplate defect score positively correlates with the diffusion of contrast medium into the disc and the severity of disc degeneration [44]. Our findings, together with published literature, suggest that endplate defects may indeed explain, in part, elevated oxygen levels in degenerate discs by reducing barriers to diffusion from the adjacent vertebral vascular and bone marrow. It is also possible that this increased diffusion leads to higher lactate levels, as circulating (serum) lactate in goats was previously reported to be $\sim 2.6 \text{ mmol}/\text{L}$ [45], which is higher than the healthy disc concentrations measured in the current study. The alterations to the NP ECM we observed histologically, including diminished proteoglycan content, also likely impact the diffusion of nutrients to resident cells [10]. Other reasons for increased metabolite levels in degenerate discs could include decreased disc height, reducing nutrient diffusion distances, and altered cellularity, impacting overall metabolic consumption rates. Consistent with our findings, increased lactate content with Pfirrmann grade has been reported by others [46, 47]. Accumulation of lactate in the disc promotes senescence and oxidative stress in NP cells, leading to apoptosis and decreased cellularity, which in turn negatively impacts the consumption of metabolites such as glucose [46]. This may in part explain the positive correlation observed between glucose and lactate concentrations.

This study had several limitations. First, we recognize that ChABC-mediated disc degeneration in goats does not fully mimic the degenerative cascade in human discs. For example, altered nutrition in human discs may be a causative factor in the initiation of the degenerative cascade, which is not recapitulated by our model. Nevertheless, we contend that it is still a valid platform for assessing relationships between the structural and compositional states of the disc and metabolite concentrations. Second, we only performed metabolite measurements at two time points, corresponding to healthy discs and those with

moderate to severe degeneration. Further, measurements were performed in a relatively small number of discs, and metabolite measurements exhibited substantial variability within study groups. A more extensive longitudinal study, incorporating intermediate time points and a larger sample size would be required to more comprehensively determine the course of metabolite changes during progressive disc degeneration. Third, while repeatability (test–retest reliability) was not formally assessed in this study, we ensured measurement stability by allowing sufficient equilibration time prior to data acquisition, averaging the results for multiple dialysates collected for each disc to reduce variability, and standardizing probe placement. Fourth, as reported previously by our group and others [17, 23, 48, 49], ChABC-induced degeneration in this model results in CEP damage and bony resorption, which in some instances is severe and associated with herniation of disc material into the adjacent vertebrae. The underlying cause is the focus of ongoing studies, but possibilities include direct enzymatic damage to the CEP or inflammation due to an immunogenic response to the ChABC protein. Importantly, the ChABC enzyme used in this study had very low endotoxin content (<0.05 endotoxin units/mL) to minimize any contaminant-driven immune response. An additional possibility is that there are intrinsic endplate weaknesses specific to some vertebrae or animals. Notably, goats have thinner CEPs compared to other species [50]. Finally, it is possible that extended surgical exposure of discs to atmospheric oxygen could have impacted results; although the fact that readings were stable for at least 60 min suggests these effects were minimal.

In summary, in this study we successfully adapted in situ techniques to assess relative NP glucose, lactate, and oxygen concentrations in a clinically relevant large animal model of disc degeneration. Our findings lay the foundation for future, more comprehensive studies, including longitudinal evaluation of disc nutrition with and without therapeutic intervention.

Author Contributions

K.R. performed experiments and data analysis, and drafted the manuscript. L.J.S. contributed to conceptual design and data analysis, and drafted the manuscript. N.R.M. contributed to conceptual design and interpretation of findings, and performed surgeries. T.P.S., M.B., and R.H. developed large animal testing concepts and equipment, and performed surgeries, imaging, and animal care. K.D.M. and J.C.O. performed experiments. R.L.M., D.M.E., G.R.D., and D.P. contributed to conceptual design and interpretation of findings. All authors reviewed and approved the manuscript prior to submission.

Acknowledgments

This study was funded by the National Institutes of Health (R01AR077435 and P30AR069619) and the Department of Veterans Affairs (I01RX001321, IK6RX003416, and IK2RX003376). We would like to acknowledge the Penn Center for Musculoskeletal Disorders MicroCT and Histology Cores for providing access to equipment. Additionally, we extend our gratitude to the staff at the Large Animal Hospital, New Bolton Center, University of Pennsylvania School of Veterinary Medicine, for their assistance during animal surgery and for managing animal care throughout the study. Furthermore, we are grateful to Dr. Todd Kilbaugh for granting access to the ISCUSflex analyzer, and we thank Jonathan Starr for his technical assistance in using this instrument. We would also like to thank Keerthana Iyer, Dong Hwa Kim, and Chenghao Zhang for their assistance with disc grading.

Disclosure

Robert L. Mauck is a former Editor-in-Chief of JOR Spine. Lachlan J. Smith and Dawn M. Elliott are members of the advisory review board of JOR Spine. They were excluded from the editorial decision-making process regarding the acceptance of this article for publication in the journal.

References

1. M. L. Ferreira, K. De Luca, L. M. Haile, et al., “Global, Regional, and National Burden of Low Back Pain, 1990–2020, Its Attributable Risk Factors, and Projections to 2050: A Systematic Analysis of the Global Burden of Disease Study 2021,” *Lancet Rheumatology* 5 (2023): e316–e329.
2. A. J. Freemont, “The Cellular Pathobiology of the Degenerate Intervertebral Disc and Discogenic Back Pain,” *Rheumatology (Oxford)* 48 (2009): 5–10.
3. J. N. Katz, “Lumbar Disc Disorders and Low-Back Pain: Socioeconomic Factors and Consequences,” *Journal of Bone and Joint Surgery, American* 88 (2006): 21–24.
4. L. J. Smith, N. L. Nerurkar, K.-S. Choi, B. D. Harfe, and D. M. Elliott, “Degeneration and Regeneration of the Intervertebral Disc: Lessons From Development,” *Disease Models & Mechanisms* 4 (2011): 31–41.
5. M. D. Humzah and R. W. Soames, “Human Intervertebral Disc: Structure and Function,” *Anatomical Record* 220 (1988): 337–356.
6. N. V. Vo, R. A. Hartman, P. R. Patil, et al., “Molecular Mechanisms of Biological Aging in Intervertebral Discs,” *Journal of Orthopaedic Research* 34 (2016): 1289–1306.
7. K. Hoffeld, M. Lenz, P. Egenolf, et al., “Patient-Related Risk Factors and Lifestyle Factors for Lumbar Degenerative Disc Disease: A Systematic Review,” *Neuro-Chirurgie* 69, no. 5 (2023): 101482, <https://doi.org/10.1016/j.neuchi.2023.101482>.
8. K. T. Weber, T. D. Jacobsen, R. Maidhof, et al., “Developments in Intervertebral Disc Disease Research: Pathophysiology, Mechanobiology, and Therapeutics,” *Current Reviews in Musculoskeletal Medicine* 8 (2015): 18–31.
9. Y.-C. Huang, J. P. Urban, and K. D. Luk, “Intervertebral Disc Regeneration: Do Nutrients Lead the Way?,” *Nature Reviews Rheumatology* 10 (2014): 561–566.
10. T. Grunhagen, A. Shirazi-Adl, J. C. Fairbank, et al., “Intervertebral Disk Nutrition: A Review of Factors Influencing Concentrations of Nutrients and Metabolites,” *Orthopedic Clinics of North America* 42 (2011): 465–477.
11. S. Rajasekaran, J. N. Babu, R. Arun, B. R. W. Armstrong, A. P. Shetty, and S. Murugan, “ISSLS Prize Winner: A Study of Diffusion in Human Lumbar Discs: A Serial Magnetic Resonance Imaging Study Documenting the Influence of the Endplate on Diffusion in Normal and Degenerate Discs,” *Spine* 29 (2004): 2654–2667.
12. L. M. Benneker, P. F. Heini, M. Alini, S. E. Anderson, and K. Ito, “2004 Young Investigator Award Winner: Vertebral Endplate Marrow Contact Channel Occlusions and Intervertebral Disc Degeneration,” *Spine* 30 (2005): 167–173.
13. A. J. Fields, A. Ballatori, E. C. Liebenberg, and J. C. Lotz, “Contribution of the Endplates to Disc Degeneration,” *Current Molecular Biology Reports* 4 (2018): 151–160.
14. C. Schizas, G. Kulik, and V. Kosmopoulos, “Disc Degeneration: Current Surgical Options,” *European Cells & Materials* 20 (2010): 306–315.
15. J. Xin, Y. Wang, Z. Zheng, S. Wang, S. Na, and S. Zhang, “Treatment of Intervertebral Disc Degeneration,” *Orthopaedic Surgery* 14 (2022): 1271–1280.
16. W. Tong, Z. Lu, L. Qin, et al., “Cell Therapy for the Degenerating Intervertebral Disc,” *Translational Research* 181 (2017): 49–58.

17. C. Zhang, S. E. Gullbrand, T. P. Schaer, et al., "Combined Hydrogel and Mesenchymal Stem Cell Therapy for Moderate-Severity Disc Degeneration in Goats," *Tissue Engineering. Part A* 27 (2021): 117–128.
18. T. Yoshikawa, Y. Ueda, K. Miyazaki, et al., "Disc Regeneration Therapy Using Marrow Mesenchymal Cell Transplantation: A Report of Two Case Studies," *Spine (Phila Pa 1976)* 35 (2010): E475–E480.
19. G. Chu, W. Zhang, F. Han, et al., "The Role of Microenvironment in Stem Cell-Based Regeneration of Intervertebral Disc," *Frontiers in Bioengineering and Biotechnology* 10 (2022): 968862.
20. K. Wuertz, K. Godburn, C. Neidlinger-Wilke, J. Urban, and J. C. Iatridis, "Behavior of Mesenchymal Stem Cells in the Chemical Microenvironment of the Intervertebral Disc," *Spine (Phila Pa 1976)* 33 (2008): 1843–1849.
21. M. G. Stovell, A. Helmy, E. P. Thelin, I. Jalloh, P. J. Hutchinson, and K. L. H. Carpenter, "An Overview of Clinical Cerebral Microdialysis in Acute Brain Injury," *Frontiers in Neurology* 14 (2023): 1085540.
22. E. Maloney-Wilensky and P. Le Roux, "The Physiology Behind Direct Brain Oxygen Monitors and Practical Aspects of Their Use," *Child's Nervous System* 26 (2010): 419–430.
23. S. E. Gullbrand, N. R. Malhotra, T. P. Schaer, et al., "A Large Animal Model That Recapitulates the Spectrum of Human Intervertebral Disc Degeneration," *Osteoarthritis and Cartilage* 25 (2017): 146–156.
24. R. J. Hoogendoorn, P. I. Wuisman, T. H. Smit, V. E. Everts, and M. N. Helder, "Experimental Intervertebral Disc Degeneration Induced by Chondroitinase ABC in the Goat," *Spine* 32 (2007): 1816–1825.
25. C. Zhang, S. E. Gullbrand, T. P. Schaer, et al., "Inflammatory Cytokine and Catabolic Enzyme Expression in a Goat Model of Intervertebral Disc Degeneration," *Journal of Orthopaedic Research* 38 (2020): 2521–2531.
26. R. Gawri, F. Mwale, J. Ouellet, et al., "Development of an Organ Culture System for Long-Term Survival of the Intact Human Intervertebral Disc," *Spine (Phila Pa 1976)* 36 (2011): 1835–1842.
27. J. T. Martin, C. M. Collins, K. Ikuta, et al., "Population Average T2 MRI Maps Reveal Quantitative Regional Transformations in the Degenerating Rabbit Intervertebral Disc That Vary by Lumbar Level," *Journal of Orthopaedic Research* 33 (2015): 140–148.
28. K. Masuda, Y. Aota, C. Muehleman, et al., "A Novel Rabbit Model of Mild, Reproducible Disc Degeneration by an Annulus Needle Puncture: Correlation Between the Degree of Disc Injury and Radiological and Histological Appearances of Disc Degeneration," *Spine* 30 (2005): 5–14.
29. E. E. McDonnell and C. T. Buckley, "Consolidating and Re-Evaluating the Human Disc Nutrient Microenvironment," *Journal of Orthopaedic Research: Spine* 5 (2022): e1192.
30. E. Liljensten, G. Skog, H. Sönnerngren, and M. Jensen-Waern, "Microdialysis as a Method for Biochemical and Physiological Studies of the Porcine and Human Disc," *Laboratory Animals* 44 (2010): 118–123.
31. M. Bue, P. Hanberg, M. B. Thomassen, et al., "Microdialysis for the Assessment of Intervertebral Disc and Vertebral Cancellous Bone Metabolism in a Large Porcine Model," *In Vivo* 34 (2020): 527–532.
32. E. M. Bartels, J. C. Fairbank, C. P. Winlove, et al., "Oxygen and Lactate Concentrations Measured In Vivo in the Intervertebral Discs of Patients With Scoliosis and Back Pain," *Spine* 23 (1998): 1–7.
33. S. R. Bibby, J. C. Fairbank, M. R. Urban, et al., "Cell Viability in Scoliotic Discs in Relation to Disc Deformity and Nutrient Levels," *Spine (Phila Pa 1976)* 27 (2002): 2220–2227.
34. S. Holm, G. Selstam, and A. Nachemson, "Carbohydrate Metabolism and Concentration Profiles of Solutes in the Canine Lumbar Intervertebral Disc," *Acta Physiologica Scandinavica* 115 (1982): 147–156.
35. A. Ejeskär and S. Holm, "Oxygen Tension Measurements in the Intervertebral Disc: A Methodological and Experimental Study," *Upsala Journal of Medical Sciences* 84 (1979): 83–93.
36. M. Fusellier, J. Clouet, O. Gauthier, et al., "Degenerative Lumbar Disc Disease: In Vivo Data Support the Rationale for the Selection of Appropriate Animal Models," *European Cells & Materials* 39 (2020): 17–48, <https://doi.org/10.22203/eCM.v039a02>.
37. R. J. Williams, L. T. Laagland, F. C. Bach, et al., "Recommendations for Intervertebral Disc Notochordal Cell Investigation: From Isolation to Characterization," *Jor Spine* 6 (2023): e1272.
38. N. R. Ekberg, N. Wisniewski, K. Brismar, and U. Ungerstedt, "Measurement of Glucose and Metabolites in Subcutaneous Adipose Tissue During Hyperglycemia With Microdialysis at Various Perfusion Flow Rates," *Clinica Chimica Acta* 359 (2005): 53–64.
39. H. Kofoed and B. Levander, "Respiratory Gas Pressures in the Spine: Measurements in Goats," *Acta Orthopaedica Scandinavica* 58 (1987): 415–418.
40. J. P. Urban, S. Smith, and J. C. Fairbank, "Nutrition of the Intervertebral Disc," *Spine (Phila Pa 1976)* 29 (2004): 2700–2709.
41. C. Nguyen-Minh, L. Riley, K.-C. Ho, et al., "Effect of Degeneration of the Intervertebral Disk on the Process of Diffusion," *AJNR. American Journal of Neuroradiology* 18 (1997): 435–442.
42. B. G. Ashinsky, E. D. Bonnevie, S. A. Mandalapu, et al., "Intervertebral Disc Degeneration Is Associated With Aberrant Endplate Remodeling and Reduced Small Molecule Transport," *Journal of Bone and Mineral Research* 35 (2020): 1572–1581.
43. U. Zehra, L. Flower, K. Robson-Brown, M. A. Adams, and P. Dolan, "Defects of the Vertebral End Plate: Implications for Disc Degeneration Depend on Size," *Spine Journal* 17 (2017): 727–737.
44. S. Rajasekaran, K. Venkatadass, J. Naresh Babu, K. Ganesh, and A. P. Shetty, "Pharmacological Enhancement of Disc Diffusion and Differentiation of Healthy, Ageing and Degenerated Discs: Results From In-Vivo Serial Post-Contrast MRI Studies in 365 Human Lumbar Discs," *European Spine Journal* 17 (2008): 626–643.
45. M. Ismail, A. A. Mahmoud, M. Y. Nasr, et al., "Clinical and Laboratory Studies on Experimentally Induced Acute Ruminal Lactic Acidosis in Male Goats," *Alexandria Journal of Veterinary Sciences* 31 (2010): 53–62.
46. Y. Zhang, L. Liu, Y. Qi, et al., "Lactic Acid Promotes Nucleus Pulposus Cell Senescence and Corresponding Intervertebral Disc Degeneration via Interacting With Akt," *Cellular and Molecular Life Sciences* 81 (2024): 24.
47. M. Radek, B. Pacholczyk-Sienicka, S. Jankowski, et al., "Assessing the Correlation Between the Degree of Disc Degeneration on the Pfirrmann Scale and the Metabolites Identified in HR-MAS NMR Spectroscopy," *Magnetic Resonance Imaging* 34 (2016): 376–380.
48. S. E. Detiger, M. N. Helder, T. H. Smit, and R. J. Hoogendoorn, "Adverse Effects of Stromal Vascular Fraction During Regenerative Treatment of the Intervertebral Disc: Observations in a Goat Model," *European Spine Journal* 24, no. 9 (2015): 1992–2000, <https://doi.org/10.1007/s00586-015-3803-7>.
49. S. Gullbrand, B. Orozco, M. Fainor, et al., "Intervertebral Disc Degeneration Instigates Vertebral Endplate Remodeling and Facet Joint Pathology in a Large Animal Model," *European Cells & Materials* 47 (2024): 125–141.
50. Y. Zhang, B. A. Lenart, J. K. Lee, et al., "Histological Features of Endplates of the Mammalian Spine: From Mice to Men," *Spine* 39 (2014): E312–E317.

Supporting Information

Additional supporting information can be found online in the Supporting Information section.